Hydrogen-Bond Cooperative Effects in Small Cyclic Water Clusters as Revealed by the Interacting Quantum Atoms Approach

8 AUTHORS, INCLUDING:

José Manuel Guevara-Vela
University of Oviedo
4 PUBLICATIONS **11** CITATIONS

Ove Christiansen
Aarhus University
184 PUBLICATIONS **7,747** CITATIONS

Tomás Rocha-Rinza
Universidad Nacional Autónoma de México
20 PUBLICATIONS **197** CITATIONS

Hydrogen-Bond Cooperative Effects in Small Cyclic Water Clusters as Revealed by the Interacting Quantum Atoms Approach

José Manuel Guevara-Vela,[a, b] Rodrigo Chávez-Calvillo,[c] Marco García-Revilla,[d] Jesús Hernández-Trujillo,[c] Ove Christiansen,[e] Evelio Francisco,[f] Ángel Martín Pendás,[f] and Tomás Rocha-Rinza*[a]

Abstract: The cooperative effects of hydrogen bonding in small water clusters $(H_2O)_n$ ($n=3–6$) have been studied by using the partition of the electronic energy in accordance with the interacting quantum atoms (IQA) approach. The IQA energy splitting is complemented by a topological analysis of the electron density ($\rho(\mathbf{r})$) compliant with the quantum theory of atoms-in-molecules (QTAIM) and the calculation of electrostatic interactions by using one- and two-electron integrals, thereby avoiding convergence issues inherent to a multipolar expansion. The results show that the cooperative effects of hydrogen bonding in small water clusters arise from a compromise between: 1) the deformation energy (i.e., the energy necessary to modify the electron density and the configuration of the nuclei of the isolated water molecules to those within the water clusters), and 2) the interaction energy (E_{int}) of these contorted molecules in $(H_2O)_n$. Whereas the magnitude of both deformation and interaction energies is enhanced as water molecules are added to the system, the augmentation of the latter becomes dominant when the size of the cluster is increased. In addition, the electrostatic, classic, and exchange components of E_{int} for a pair of water molecules in the cluster $(H_2O)_{n-1}$ become more attractive when a new H_2O unit is incorporated to generate the system $(H_2O)_n$ with the last-mentioned contribution being consistently the most important part of E_{int} throughout the hydrogen bonds under consideration. This is opposed to the traditional view, which regards hydrogen bonding in water as an electrostatically driven interaction. Overall, the trends of the delocalization indices, $\delta(\Omega,\Omega')$, the QTAIM atomic charges, the topology of $\rho(\mathbf{r})$, and the IQA results altogether show how polarization, charge transfer, electrostatics, and covalency contribute to the cooperative effects of hydrogen bonding in small water clusters. It is our hope that the analysis presented in this paper could offer insight into the different intra- and intermolecular interactions present in hydrogen-bonded systems.

Keywords: cooperative effects · electrostatic interactions · exchange interactions · hydrogen bonds · quantum atoms

Introduction

Hydrogen bonding (HB) is arguably the most important intermolecular interaction. It has been recognized in a wide range of phenomena: it determines the conformation, aggregation, and dynamics of many systems in biochemistry,[1–3] supramolecular chemistry,[4] and crystal engineering,[5] to mention only a few. Most significantly, hydrogen bonding is responsible for the properties of water in the condensed phase both in pure form and as a solvent.

The versatility of hydrogen bonding has made it difficult to attain a simple definition for it. Recently, IUPAC has suggested that a typical hydrogen bond, X—H⋯Y—Z, is an intra- or intermolecular attractive interaction in which there

[a] J. M. Guevara-Vela, Prof. Dr. T. Rocha-Rinza
    Instituto de Química, UNAM, Circuito Exterior
    Ciudad Universitaria, Delegación Coyoacán C.P. 04510
    Mexico City (Mexico)
    Fax: (+52) 555-616-2217
    E-mail: tomasrocharinza@gmail.com

[b] J. M. Guevara-Vela
    Present address: Institut de Ciencia Molecular
    Parc Científic, Universitat de València
    Catedrático José Beltrán, 2. 46980 València (Spain)

[c] R. Chávez-Calvillo, Prof. Dr. J. Hernández-Trujillo
    Departamento de Física y Química Teórica
    Facultad de Química, UNAM, México D.F.
    04510, Mexico City (Mexico)

[d] Prof. Dr. M. García-Revilla
    Departamento de Química
    División de Ciencias Naturales y Exactas
    Universidad de Guanajuato, 36050
    Guanajuato, Guanajuato (Mexico)

[e] Prof. Dr. O. Christiansen
    Center for Oxygen Microscopy and Imaging
    Department of Chemistry, University of Aarhus
    Langelandsgade 140, 8000, Århus C (Denmark)

[f] Prof. Dr. E. Francisco, Prof. Dr. Á. Martín Pendás
    Departamento de Química Física y Analítica
    Universidad de Oviedo, 33006 Oviedo (Spain)

Supporting information for this article is available on the WWW under http://dx.doi.org/10.1002/chem.201300656.

Abstract in Spanish: *Se estudian los efectos cooperativos del Enlace de Hidrógeno (EH) en cúmulos de agua pequeños $(H_2O)_n$ (n=3–6) mediante la partición de la energía electrónica que proporciona el método de Átomos Cuánticos Interactuantes (ACI). La división de la energía electrónica propuesta por ACI es complementada con el análisis topológico de la densidad electrónica ($\rho(\vec{r})$)) de la Teoría Cuántica de Átomos en Moléculas (TCAEM) y con el cálculo de la energía electrostática que se basa en integrales mono y bielectrónicas, evitando así los problemas de convergencia inherentes a una expansión multipolar. Los resultados muestran que los efectos cooperativos del EH en cúmulos de agua pequeños surgen de un compromiso entre: 1) la energía de deformación, es decir, la energía necesaria para convertir la densidad electrónica y la configuración de los núcleos de una molécula de agua aislada en aquellas dentro de cada uno de los cúmulos moleculares y 2) la energía de interacción de esas moléculas deformadas en los sistemas (H_2O). La magnitud de ambas cantidades aumenta con el tamaño del sistema, aunque el incremento de la energía de interacción es mayor que el de la energía de deformación cuando se añaden moléculas al cúmulo molecular. Adicionalmente, las componentes clásica, de intercambio y electrostática de la energía de interacción para un par de moléculas de agua en el cúmulo $(H_2O)_{n-1}$ se vuelven más atractivas cuando una molécula de agua es incorporada para generar el sistema $(H_2O)_n$, siendo la contribución de intercambio la más importante. Esto se opone a la interpretación tradicional que considera que el EH es una interacción esencialmente electrostática. En resumen, las tendencias de los índices de deslocalización $\delta(\Omega,\Omega')$, las cargas de TCAEM, la topología de $\rho(\vec{r})$ y los resultados de ACI muestran conjuntamente cómo la polarización, la transferencia de carga, así como las interacciones electrostáticas y covalentes contribuyen a los efectos cooperativos del EH en cúmulos de agua pequeños. Esperamos que el análisis mostrado en este artículo pueda proporcionar un nuevo entendimiento acerca de las distintas interacciones intra e intermoleculares que se presentan en sistemas con EHs.*

are indications for the formation of a bond between H and Y, and X is more electronegative than H.[6] There are several structural, electronic, spectroscopic, and thermodynamic criteria for the characterization of an interaction as a hydrogen bond, which might not be observed in particular cases and hence will lead to a subjective assessment of borderline cases.[6] Other definitions consider that a hydrogen bond X—H⋯Y—Z entails a proton donation from X—H to Y—Z,[7] and that the fundamental feature of the interaction is the attraction of the hydrogen atom by two atoms X and Y, so that hydrogen acts as a bridge between them.[5] Despite the different definitions of a hydrogen bond, there is a general agreement on its anisotropic character, geometric requirements, and energy interval.[5,7] Depending on the nature of X, Y and Z, a hydrogen bond involves covalent, polarization, electrostatic, and van der Waals interactions in differ-

ent proportions.[8] It is not generally possible to state that every hydrogen bond is dominated by one or another common contribution.[7] Non-additivity, a major feature of hydrogen bonding, results from the aforementioned non-electrostatic interactions. Thus, there can be cooperative effects in a network of hydrogen bonds. In a chain with two hydrogen bonds, A—H⋯B—H⋯C, both HBs strengthen each other.[9] These effects are not restricted to only two hydrogen bonds and they have been described in water chains that contain from two to an infinite number of molecules.[10]

In connection with the previous discussion, there has been recent interest in water clusters,[11–15] which have become an archetype of hydrogen-bonding cooperative effects.[8,16–21] This can be realized, for example, in the exponential reduction of the intermolecular distance between oxygen atoms[16] and the redshift of the hydrogen-bonded OH stretching vibrational frequency as a function of the cluster size.[16] Theoretical and experimental results agree in the description of these trends.[8,16,22] Besides giving insights into the cooperative effects and the dynamics of hydrogen bonding as well as the arrangements of H_2O molecules that occur in the condensed phase,[16] the study of water clusters is linked with several important processes such as the creation of acid rain,[23,24] spontaneous water droplet nucleation in the gas phase,[25] ion production and activity in aqueous solution,[26] and the climate-relevant infrared absorption[27,28] in the atmosphere.

The cooperative effects of hydrogen bonding in water clusters are not fully understood. Many-body induction as well as charge transfer have been proposed to be the main reasons for such effects.[9,16] Most of the explanations offered so far rely on more or less arbitrary procedures to extract these energetic components from electronic structure calculations.[29–32] It is our opinion that real-space procedures might shed new light on these matters to narrow down the origin of cooperativity by providing orbital-invariant results that are independent from external references. This paper aims to give a detailed real-space account of the contributions to the interaction energy among water molecules in the formation of the water dimer and small cyclic water clusters $(H_2O)_n$ with $n = 3$–6 (see Figure 1) to provide insight into the cooperative effects of hydrogen bonding. The pres-
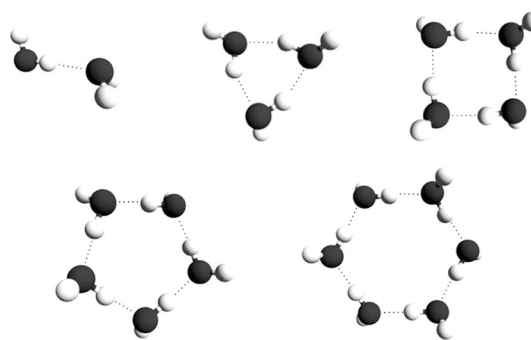

Figure 1. Water dimer and small cyclic water clusters considered in this work.

ent study is restricted to systems that contain only homo-dromic cycles of hydrogen bonds, that is, cyclic structures that comprise only single HB donors and acceptors in which all the hydrogen bonds run in the same direction as schematized in Figure 2 a. This is because homodromic cycles are
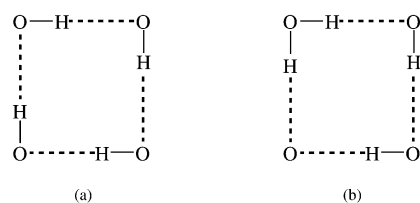

Figure 2. a) Homodromic and b) antidromic cycles of hydrogen bonds.

related only to cooperative effects of hydrogen bonding, whereas antidromic cycles (Figure 2b) are also associated with local anticooperative effects due to the presence of double donors and acceptors of hydrogen bonding within these structures.[7] In addition, the interaction energies among H_2O molecules in water hexamers that contain homodromic and antidromic cycles are strongly dependent upon the single or double nature of the hydrogen-bonding donors and acceptors.[33] This hinders a direct comparison with smaller water clusters that comprise a single homodromic cycle. The ring-shaped water hexamer studied in this work has a structure reminiscent of a chair conformation of cyclohexane; it is the most stable isomer of the water hexamers, made up of only one homodromic cycle, unlike, for example, the boat or twisted-boat water hexamers, as shown by different electronic structure calculations that include CCSD(T), MP2, and DFT methods.[34–36] Our emphasis is on a qualitative analysis of cooperative effects of hydrogen bonding. For recent efforts to construct highly accurate potentials for small water clusters, we refer to the work of Szalewicz et al.[37] and Wang et al.[38] The energy analysis presented in this work is in compliance with the interacting quantum atoms (IQA)[39, 40] approach, which can be used to study covalent and noncovalent interactions on the same footing,[41–44] thereby providing energetic quantities with an straightforward physical meaning based exclusively upon the first- and second-order reduced density matrices of the system under scrutiny.[39, 40] In this way, IQA is devoid of the intrinsic arbitrariness of other energy-partitioning procedures, for example, those which rely upon orbital-dependent quantities. More importantly, this approach has been used in insightful studies of intra-[45] and intermolecular[46–48] noncovalent interactions and chemical bonding in general.[49–51] That is why it was decided to use this approach to obtain a further understanding of the cooperativity of hydrogen bonding in small water clusters in terms of physically meaningful contributions, thereby providing a new description of the phenomenon. Furthermore, an evaluation of the electrostatic energy within water clusters by employing mono- and bielectronic integrals to further dissect the interaction energy among the constituent monomers, as well as a topo-logical analysis of the electron density ($\rho(\mathbf{r})$) and the calculation of selected properties on the basis of the quantum theory of atoms-in-molecules (QTAIM), were also performed.

First, the topological analysis of $\rho(\mathbf{r})$, the properties of the atoms-in-molecules as defined by QTAIM, the IQA approach, and the calculation of the electrostatic energy by means of mono- and bielectronic integrals are briefly reviewed. Then, the details of the calculations carried out in this work are given, and the cooperative effects of hydrogen bonding in small water clusters are discussed in the light of the results of this investigation. Finally, some concluding remarks are highlighted. Overall, this study shows how electrostatics, polarization, charge transfer, and covalent bonding combine to create the cooperative effects of hydrogen bonding within small water clusters, thereby providing further insight into the intramolecular and intermolecular interactions present in a hydrogen bond.

Computational Methods

QTAIM is a tool of common use in organic and inorganic theoretical chemistry[52–56] because the concepts developed in this theory—such as atom, functional group, chemical structure, as well as electronic localization and delocalization—have been successfully associated with corresponding basic ideas of traditional chemistry. The topology of $\rho(\mathbf{r})$ can be associated with different elements of molecular structure, such as the presence of cyclic and caged backbones, and particularly to chemical bonding,[57] although this issue has caused controversy in the literature.[58–60] According to QTAIM, the physical space of an electronic system can be divided into disjoint regions Ω associated with the atoms of chemistry for which the average value of quantum observables relevant to this study such as charge and dipole moment can be calculated in a routine way.[61, 62] In addition, QTAIM defines electron localization and delocalization indexes represented by $\lambda(\Omega)$ and $\delta(\Omega,\Omega')$ respectively, in terms of the properties of the Fermi and Coulomb holes.[63, 64] Particularly important for this work is the concept that the larger the delocalization index $\delta(\Omega,\Omega')$, the more covalent the interaction between the atoms Ω and Ω',[65] and therefore $\delta(\Omega,\Omega')$ is useful for characterizing both intra- and intermolecular interactions.

The QTAIM-based splitting of the real space into disjoint atoms A, B, and so on, each one of which contains one nucleus, allows one to rewrite the electronic energy within the non-relativistic Born–Oppenheimer approximation as a sum of atomic net (E_{net}^{A}) and interaction energies (E_{int}^{AB})[39, 40] in the form [Eq. (1)]:

$$E = \sum_A E_{net}^A + \sum_{A>B} E_{int}^{AB}$$
$$= \sum_A (T^A + V_{ne}^{AA} + V_{ee}^{AA}) + \sum_{A>B} (V_{nn}^{AB} + V_{ne}^{AB} + V_{ne}^{BA} + V_{ee}^{AB}) \qquad (1)$$

in which a self-explanatory notation is used. The division of the real space implicit in Equation (1) can be performed by means of different methods, which include those of Bader,[61] Hirshfeld,[66] and Becke[67] fuzzy atoms. The full expressions of the terms of Equation (1) are given in the literature.[68] This equation constitutes the basis upon which the IQA energy partition is built.

A feature of the IQA approach that is particularly important for this work is the possibility of gathering atoms in groups, $\mathscr{G}$, $\mathscr{H}$, and so forth. The group energy $E_{net}^{\mathscr{G}}$ contains all atomic net energies plus the interaction energies among all the pairs of atoms inside the group $\mathscr{G}$. The energy E in terms of group net and interaction energies is then also given by Equation (1), but by exchanging the atomic labels A and B for the

group labels $\mathcal{G}$ and $\mathcal{H}$, respectively. Another important concept for this study is that of the deformation energy: if the groups $\mathcal{G}$, $\mathcal{H}$, $\mathcal{I}$, and so forth represent isolated chemical species, then the energy associated with the formation of a molecular cluster $\mathcal{G}\cdots\mathcal{H}\cdots\mathcal{I}\cdots$A through the process $\mathcal{G}+\mathcal{H}+\mathcal{I}+\ldots\rightleftharpoons\mathcal{G}\cdots\mathcal{H}\cdots\mathcal{I}\cdots$, reads [Eq. (2)]:

$$\Delta E = E^{\mathcal{G}\cdots\mathcal{H}\cdots\mathcal{I}\cdots} - (E_{iso}^{\mathcal{G}} + E_{iso}^{\mathcal{H}} + E_{iso}^{\mathcal{I}} + \ldots) = \sum_{\mathcal{G}} E_{def}^{\mathcal{G}} + \sum_{\mathcal{G}>\mathcal{H}} E_{int}^{\mathcal{G}\mathcal{H}} \quad (2)$$

in which $E_{iso}^{\mathcal{G}}$ represents the energy of the isolated fragment $\mathcal{G}$, whereas $E_{def}^{\mathcal{G}} = E_{net}^{\mathcal{G}} - E_{iso}^{\mathcal{G}}$ denotes the deformation energy of the same species, which is the energy related to the concomitant distortion of its nuclear framework and electron density when it interacts with the rest of the species in the molecular cluster.

Further insight into the intra- and intermolecular interactions can be obtained by considering the splitting of the pair density (ρ_2) in its coulombic (ρ_2^C), and exchange-correlation (ρ_2^{xc}) components, $\rho_2(\mathbf{r}_1,\mathbf{r}_2) = \rho_2^C(\mathbf{r}_1,\mathbf{r}_2) + \rho_2^{xc}(\mathbf{r}_1,\mathbf{r}_2)$[68] This partitioning enables one to separate the electron–electron interaction between two different atoms A and B into Coulomb (C) and exchange-correlation (xc) components, $V_{ee}^{AB} = V_C^{AB} + V_{xc}^{AB}$ and the interaction energy into a classical (i.e., coulombic), $V_{cl}^{AB} = V_C^{AB} + V_{ne}^{AB} + V_{ne}^{BA} + V_{nn}^{AB}$, and a purely quantum-mechanical (i.e., exchange-correlation) term, V_{xc}^{AB}, so that [Eq. (3)]:

$$E_{int}^{AB} = V_{cl}^{AB} + V_{xc}^{AB} = V_{cl}^{AB} + V_X^{AB} + V_{corr}^{AB} \quad (3)$$

in which the exchange-correlation term is further divided into exchange (V_X^{AB}) and correlation (V_{corr}^{AB}) contributions. The above partition of ρ_2 may also be used to divide the electron–electron interaction between two different groups ($V_{ee}^{\mathcal{G}\mathcal{H}}$) into a Coulomb ($V_C^{\mathcal{G}\mathcal{H}}$) and an exchange-correlation term ($V_{xc}^{\mathcal{G}\mathcal{H}}$). This implies that Equation (3) remains valid when the labels A and B are replaced by $\mathcal{G}$ and $\mathcal{H}$. Similarly, the quantity $V_{cl}^{\mathcal{G}\mathcal{H}} = V_C^{\mathcal{G}\mathcal{H}} + V_{ne}^{\mathcal{G}\mathcal{H}} + V_{ne}^{\mathcal{H}\mathcal{G}} + V_{nn}^{\mathcal{G}\mathcal{H}}$ represents the classical interaction between the charge (nuclear+electron) distributions of both groups and includes electrostatic, polarization, and charge-transfer effects,[69] whereas $V_{xc}^{\mathcal{G}\mathcal{H}}$ is traditionally associated with covalent (exchange) and electron correlation interactions.

In the case of the study of molecular clusters, it is possible to additionally dissect the interaction energy by calculating separately the electrostatic contribution (ele) among the distinct fragments inside a molecular cluster from their unperturbed electron densities. For a bimolecular noncovalent cluster this contribution is given by [Eq. (4)]:

$$E_{ele} = \int\int \rho_T^{\mathcal{G}}(\mathbf{r}_1)\rho_T^{\mathcal{H}}(\mathbf{r}_2)r_{12}^{-1}d\mathbf{r}_1 d\mathbf{r}_2 \quad (4)$$

in which $\rho_T^{\mathcal{G}}(\mathbf{r}) = \Sigma_{A\in\mathcal{G}}Z_A\delta(\mathbf{r}-\mathbf{r}_A) - \rho^{\mathcal{G}}(\mathbf{r})$ is the total (nuclear plus electron) density of the group $\mathcal{G}$, with an equivalent definition for $\rho_T^{\mathcal{H}}(\mathbf{r})$, and $\rho^{\mathcal{G}}(\mathbf{r})$ is the electron density of the isolated species $\mathcal{G}$. We should note at this point that Equation (4) for E_{ele} coincides with ΔE_{elstat}, the quasiclassical Coulomb interaction between the frozen charge densities of two fragments within the energy decomposition analysis (EDA) methodology,[70–74] and also that the $\mathbf{r}_1(\mathbf{r}_2)$ coordinate in Equation (4) is not restricted to take values inside the set of QTAIM basins that correspond to group $\mathcal{G}$ ($\mathcal{H}$); that is, the integrations in Equation (4) are extended to the whole space. The procedure used in this work to obtain E_{ele} is described in the Appendix.

Computational details: The geometries of the systems shown in Figure 1 were optimized by using the MP2 approximation[75] along with the aug-cc-pVTZ[76] basis set as implemented in the quantum chemistry package GAMESS-US.[77] This methodology has been successfully used to describe the geometry of hydrogen-bonded systems.[78] To assess the effects of electron correlation in the cooperative effects of hydrogen bonding in small water clusters, we performed single-point calculations and geometry optimizations of the molecular clusters of interest for this study by using the CCSD/aug-cc-pVTZ and HF/aug-cc-pVTZ approximations, respectively. The geometries for the CCSD calculations were taken from the literature.[79] The calculation of the harmonic frequencies showed that

the results of the geometry optimizations are local minima on the corresponding potential energy hypersurfaces.

The partitions of the energy by using the IQA approach were carried out with the aid of the PROMOLDEN[80] program at the HF/aug-cc-pVTZ level of theory, because this methodology qualitatively accounts well for the cooperative hydrogen-bonding effects in small water clusters (see below). In this regard, the inclusion of electron correlation in IQA can nowadays only be done through FCI or complete active space SCF (CASSCF) calculations. Although the former method is not feasible for the systems and basis sets considered in this work, the application of the latter is discouraged by the absence of static correlation in small water clusters. With regard to density functional and density matrix functional theory, there is not a generally accepted way to approximate the pair density from the electron density or the first-order reduced density matrix to carry out an IQA energy decomposition.[81]

The analysis of the topology of the electron density and the calculation of the properties of the atoms in the molecules were carried out with the AIMALL[62] package. Finally, the calculation of the electrostatic energy was carried out with the MOLPRO program.[82] The structures of the water clusters utilized for the calculation of E_{ele} in Equation (10) in the Appendix were obtained through an HF/aug-cc-pVTZ geometry optimization by using frozen monomers with the experimental geometry since the calculation of the electrostatic energy requires the unperturbed electron density of the interacting molecules. The data were visualized using GNUPLOT 4.2[83] and AVOGADRO 1.0.3.[84]

Results and Discussion

Cooperative effects of hydrogen bonding from sequential formation energies: Figure 3 shows the difference [Eq. (5)]:

$$\Delta\Delta E = \Delta E_n - \Delta E_2 \quad (5)$$

in which ΔE_n is the change in energy for the process $(H_2O)_{n-1} + H_2O \rightleftharpoons (H_2O)_n$ ($n=2$–6) at several levels of com-
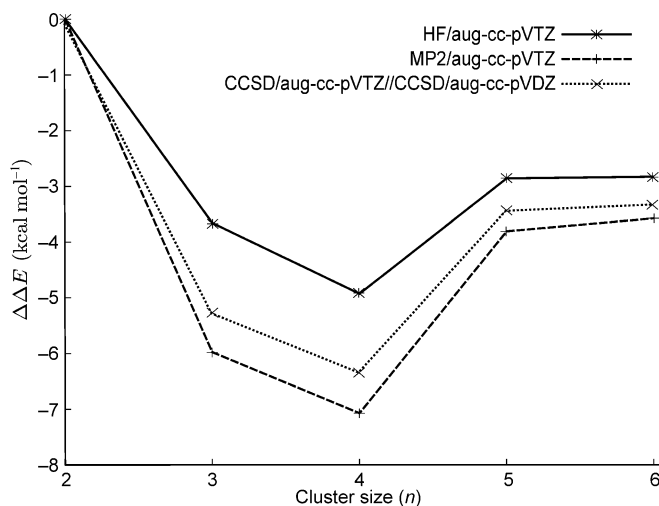

Figure 3. Comparison between the energies associated with 1) the inclusion of a water molecule to the system $(H_2O)_{n-1}$ to form the water cluster $(H_2O)_n$ (i.e., $(H_2O)_{n-1} + H_2O \rightleftharpoons (H_2O)_n$ with $n=2$–6) and 2) the formation of the isolated hydrogen bond in $(H_2O)_2$ (i.e., $H_2O + H_2O \rightleftharpoons (H_2O)_2$). The value of $\Delta\Delta E$ is calculated in accordance with Equation (5) at different levels of theory. The more negative the value of $\Delta\Delta E$, the stronger the cooperative effects of hydrogen bonding in the formation of the $(H_2O)_n$ cluster.

putation. A negative value of $\Delta\Delta E$ means that the inclusion of the nth water molecule to generate the water cluster $(H_2O)_n$ is energetically more favorable than the formation of an isolated hydrogen bond in the water dimer. Thus, $\Delta\Delta E < 0$ indicates cooperative effects in the network of hydrogen bonding within $(H_2O)_n$: the more negative this value, the larger the hydrogen-bonding cooperative effects in the formation of the $(H_2O)_n$ cluster. As can be seen in Figure 3, $\Delta\Delta E$ is negative for $n = 3$–6, thus evidencing the cooperative effects of hydrogen bonding in small water clusters. The more negative values for $\Delta\Delta E$ in Figure 3 are for the water trimer and tetramer. Such nonadditive effects are also present in the generation of the water pentamer and hexamer, although to a smaller degree. The HF (MP2) approximation underestimates (overestimates) the magnitude of $\Delta\Delta E$ relative to the CCSD method, which provides the best assessment of electron correlation considered in this work.[85] Indeed, Figure 3 shows that it is necessary to consider electron correlation to quantitatively account for the cooperative effects of hydrogen bonding in small H_2O clusters; nevertheless, it is also evident that the HF approximation qualitatively describes the phenomenon. Similarly, the inclusion of electron correlation does not change the IQA description of distinct hydrogen-bonded systems,[46] and therefore the HF methodology was used along with the IQA method to gain further insight into the cooperative effects of hydrogen bonding in H_2O clusters.

Deformation and interaction energies: This section discusses the importance of the deformation (E_{def}) and interaction (E_{int}) energies within small water clusters $(H_2O)_n$ ($n = 2$–6). We start by considering the formation of the water trimer from the addition of an H_2O molecule to $(H_2O)_2$ as schematized in Figure 4. This process increases the deformation and
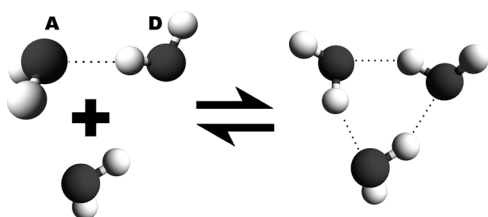

Figure 4. Formation of the water trimer from the interaction of a water molecule with $(H_2O)_2$.

net energies of the water monomers with respect to those in the water dimer, as shown in Figure 5 for $n = 2$ and 3. Nonetheless, there is an enlargement in the magnitude of the attractive interaction of the water molecules within the water trimer when an additional molecule interacts with the cluster $(H_2O)_2$. This is in accordance with the charge transfer that occurs in $(H_2O)_2$[9] in which the proton donor (molecule D in Figure 4) accepts a small amount of electron density from the proton acceptor (molecule A in the same Figure). The slight excess amount of negative charge on molecule D
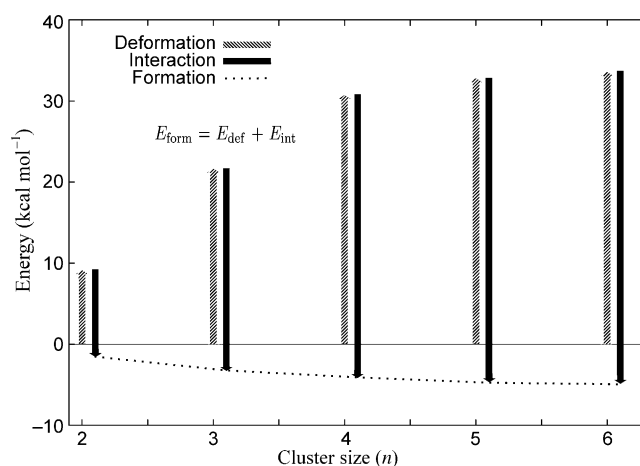

Figure 5. Deformation, interaction, and formation energies per water molecule as a function of the size of the system for clusters $(H_2O)_n$ in which $n = 2$–6.

makes it a better proton acceptor than an isolated water molecule. Concomitantly, the hydrogen atoms of the electron-deficient molecule A are more acidic than those of one isolated H_2O molecule and thus more liable to participate in a hydrogen bond. The increase in the magnitude of E_{int} and E_{def} remains for water clusters larger than the trimer. The rise in the deformation energy along with the size of the water cluster indicates an alteration of the electron density for the water molecules within $(H_2O)_n$ relative to an isolated H_2O molecule. The importance of the rearrangement of water molecules as a consequence of hydrogen bonding had been previously noted by Devereux and Popelier.[12] This change in $\rho(\mathbf{r})$ is more pronounced as water molecules are added to the system and is in agreement with the monotonic increase of the average dipole moment of a water monomer within a given cluster, from 1.99 D (the experimental gas-phase value is 1.86 D[86]) in an isolated H_2O molecule to 2.56 D in $(H_2O)_6$ as presented in Figure 6. Moreover, this

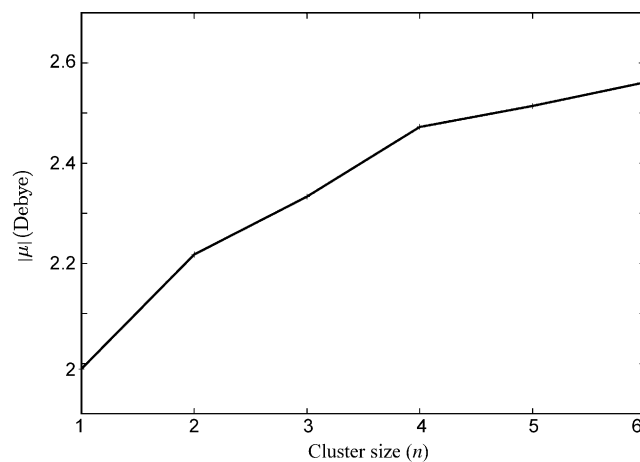Figure 6. Average dipole moment of a water monomer within a small water cluster $(H_2O)_n$ with $n = 2$–6.

deformation of the electron density of water molecules is even larger in the condensed phase: the dipole moment of liquid water is about 60% larger (2.9–3.0 D[87,88]) than the corresponding value in the gas phase.

The rate of increase of E_{def} and E_{int} with the size of the cluster in Figure 5 is also noteworthy. Both quantities increase rapidly until the water tetramer and then their magnitudes increase slightly in $(H_2O)_5$ and $(H_2O)_6$. Previous work showed that the deformation energy in $(H_2O)_2$ is related to the antisymmetrization of the wavefunction of the cluster written as a product of the wavefunctions of the constituent monomers (i.e., to the enlargement of the dimension of the fermionic Fock space).[46] The proportionality of the deformation energy of a monomer and the intermonomer interaction energy has been noticed in the past.[89,90] Nonetheless, the definition of the deformation energy in previous studies is different to that used in this work in which a real-space decomposition technique is considered to obtain a detailed, uniform analysis of all the components of the deformation and interaction energies in an attempt to open a new window on the origin of cooperativity of hydrogen bonding. The changes on E_{def} and E_{int} are larger when there are water molecules arranged in a branched configuration, for example, upon going from $(H_2O)_2$ to $(H_2O)_3$ in Figure 5. The water trimer consists of a cycle of charge polarization, which is absent in $(H_2O)_2$ and in which the magnitude of the atoms-in-molecules charges that correspond to the oxygen and the hydrogen-bonded hydrogen ($H_{bonding}$) atoms increase monotonically, that is, $H_{bonding}$ atoms transfer electron density to the oxygen atoms as water molecules are added to the system, as can be seen in Table 1. On the other hand, the atomic charges and energies of the hydrogen

served in Figure 6 in which the change in intraatomic dipole moments are counteracted,[12] but also accounts for the considerable deformation energy shown in Figure 5. The correspondence between this polarization and the deformation energy is illustrated in Figure 7, which indicates a strong cor-
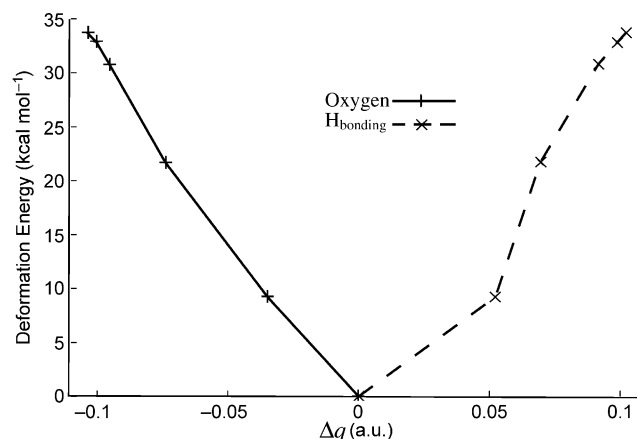

Figure 7. Correlation between the deformation energy of a water monomer within a small water cluster and the change in the atomic charge of the bonding hydrogen and oxygen atoms with respect to the values in an isolated H_2O molecule.

relation between E_{def} and the charges in O and $H_{bonding}$. At the same time, this polarization increases the interaction among H_2O molecules constituting the cluster, as discussed in the next section. In this sense, there is a near-complete conversion of E_{def} into E_{int}. The QTAIM energies indicate that the oxygen atoms increase their stability with the size of the cluster, whereas $H_{bonding}$ shows the opposite behavior: there is a prevalence of the former effect over the latter.

The augmentation of the attractive interaction among water molecules within a small H_2O cluster more than compensates the enlargement of the deformation energies in all the systems considered in this study. Figure 5 shows that the sum $E_{int} + E_{def}$, with the sum-

Table 1. Average of 1) the electron density at $(3,-1)$ critical points associated with the hydrogen bond and the intramonomer O−$H_{bonding}$ covalent bond as well as 2) the atomic charges and energies for the atoms involved in this interaction (O and $H_{bonding}$) within small $(H_2O)_n$ clusters in which $n = 2$–6. Atomics units are used throughout.

n	$\rho_{bcp}(O\cdots H_{bonding})$	$\rho_{bcp}(O-H_{bonding})$	$q(O)$	$E(O)$	$q(H_{bonding})$	$E(H_{bonding})$
2	0.0262	0.3636	−1.3000	−75.4264	0.6853	−0.2983
3	0.0298	0.3527	−1.3391	−75.4558	0.7025	−0.2837
4	0.0412	0.3408	−1.3605	−75.4729	0.7247	−0.2678
5	0.0446	0.3379	−1.3655	−75.4770	0.7320	−0.2626
6	0.0451	0.3377	−1.3690	−75.4796	0.7353	−0.2605

atoms that do not participate in a hydrogen bond (H_{free}) change less than 5 millielectrons and 3 mHa, respectively, upon going from $(H_2O)_2$ to $(H_2O)_6$. The saturation of the properties of the oxygen and $H_{bonding}$ atoms occurs more slowly: in contrast to H_{free}, the $H_{bonding}$ (O) atomic charge and energy change by 50 millielectrons and 62 mHa (69 millielectrons and 73 mHa), respectively, in $(H_2O)_6$ with respect to $(H_2O)_2$, thereby evidencing the fact that the effects of hydrogen bonding are mainly exerted on the atoms that comprise the rings shown in Figure 1 i.e., the O and $H_{bonding}$ atoms. The polarization of the oxygen and the hydrogen-bonding atoms not only is the main reason for the trend ob-

mands having opposite signs, becomes more negative as water molecules are incorporated into the system, and therefore the magnitude of the resulting formation energy per water molecule increases along with the size of the cluster, although it is notably smaller in magnitude than the deformation and interaction energies. In other words, the cooperative effects of hydrogen bonding within small water clusters are a consequence of the partial cancellation of the two substantially larger contributions shown in Figure 5, namely, the increase in both E_{def} and E_{int}, with the latter being dominant. Now that we have established the relative importance of the deformation and interaction energies in

the formation of small water clusters, the next section considers the dissection of E_{int} into its different components.

Electrostatic, classical, and exchange contributions to the interaction energies: The interaction energy decomposition among the monomers in the water clusters $(H_2O)_n$ addressed in this work in its classical and exchange components shows that the attractive character of both contributions increases along with the size of the cluster as displayed in Figure 8. In addition, $|V_X|$ is considerably larger than $|V_{cl}|$, which indicates that the former is the most important
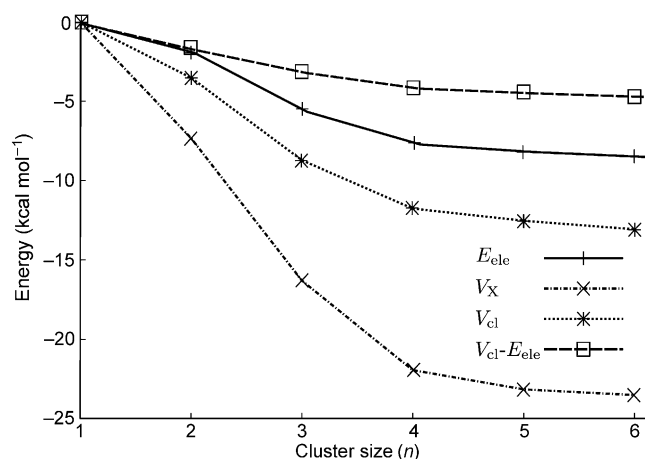

Figure 8. Electrostatic (E_{ele}), classical (V_{cl}), and exchange (V_X) contributions of the interaction energy per water molecule within small water clusters $(H_2O)_n$ with $n = 2$–6. The difference $V_{cl} - E_{ele}$, which accounts for polarization and charge-transfer effects, is presented as well.

component in the interaction energy in the clusters shown in Figure 1. This implies that the hydrogen bond in small water clusters is propelled by exchange in opposition to the widespread view that other components, particularly electrostatics, govern this interaction. The results of the correlated calculations in Figure 3 suggest that the component V_{xc} should be even more attractive than V_X.

Figure 8 shows as well that the electrostatic energy E_{ele}, calculated through Equation (11), becomes more attractive as the size of the cluster increases. Since E_{ele} is strongly dependent on orientation, the rise in this component of the interaction energy is related with that of the O−H···O angle from 150.9° in $(H_2O)_3$ to 178.5° in $(H_2O)_6$. It can also be observed that the difference $V_{cl} - E_{ele}$, which takes into account the polarization and charge-transfer effects on the interaction energy increases as water molecules are incorporated into the system. The augmentation of $|V_{cl} - E_{ele}|$ is consistent with the increase in the dipole moment of the water monomers with the size of the system shown in Figure 6 and the QTAIM charge analysis in Table 1. This enhances the attractive character of V_{cl}, but does not change E_{ele} since the latter is obtained by considering the unperturbed electron densities of the monomers.[91]
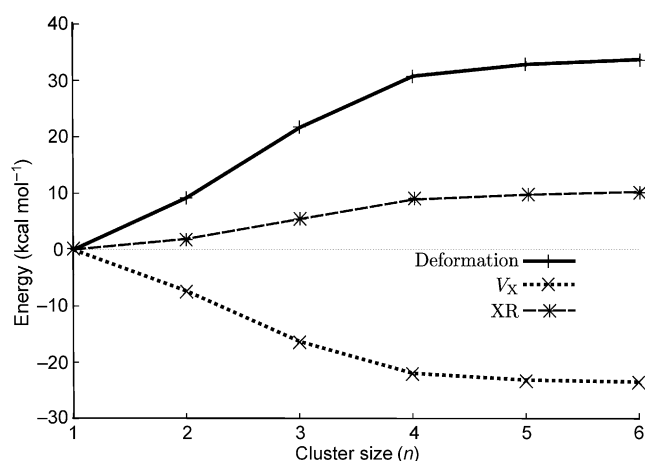

Figure 9. Deformation, exchange, and XR $= V_X - E_{def}$ per water molecule within small water clusters $(H_2O)_n$ with $n = 2$–6.

Another relevant descriptor is the exchange repulsion XR $= V_X + E_{def}$,[46] which is associated with a similar concept in the EDA energy partition. Figure 9 shows that XR increases with the number of water molecules in the system, and therefore the cooperative effects of hydrogen bonding in water clusters are accompanied by a rise in exchange repulsion. This is in contrast to foregoing results that indicate that there is an effective partial cancellation between deformation and exchange energies, thereby resulting in almost zero values for XR in hydrogen-bonded systems.[46] Finally, it should be mentioned that the rate of change for the contributions to the interaction energy shown in Figure 8 is qualitatively similar and in accordance with that of E_{def} and E_{int} in Figure 5, which indicates a saturation of the components of the interaction energy for $(H_2O)_5$ and $(H_2O)_6$.

The analysis of the intermolecular interactions within the water dimer and cyclic $(H_2O)_n$ clusters ($n = 3$–6) can also be carried out by considering atomic pairs in which each atom forms part of a different monomer. Figure 10 shows the atom numbering used for the corresponding discussion of $(H_2O)_2$ and Table 2 reports the classical and exchange contribution of the interaction energies between 1) an atom in molecule D and 2) another atom of molecule A in $(H_2O)_2$ (see the left part of Figure 4). First, there is an important contribution of every pair of intermolecular atoms to the classical component of the interaction energy. There is a reduction in V_{cl} due to the intermolecular pairs formed by an oxygen and a hydrogen atom in different molecules. This is to be contrasted with an increase in V_{cl} because of the intermolecular pairs in which both atoms are either oxygen or hydrogen.
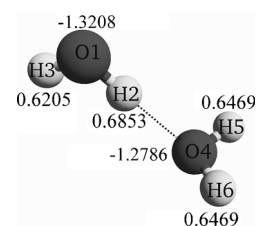

Figure 10. Atom numbering in $(H_2O)_2$ for the discussion of the intermolecular atom pair interactions within this cluster. QTAIM charges are shown in atomic units as well.

Table 2. Classical and exchange interactions for every intermolecular atom pair in the water dimer. The atom numbering is shown in Figure 10 and atomic units are used throughout.

Atom pairs	V_{cl}	V_X
O1−O4	0.306120	−0.009494
O1−H5	−0.140870	−0.000061
O1−H6	−0.140874	−0.000061
H2−O4	−0.219283	−0.013496
H2−H5	0.096684	−0.000074
H2−H6	0.096687	−0.000074
H3−O4	−0.125232	−0.000094
H3−H5	0.057772	0.000000
H3−H6	0.057773	0.000000

Figure 11. Exchange component of the interaction energy between 1) contiguous oxygen atoms (O···O) and 2) an oxygen and a hydrogen atom involved in a hydrogen bond within the clusters $(H_2O)_n$ with $n=2–6$.

The contributions of the intermolecular atom pairs to the classical component of the interaction energy are consistent with the QTAIM charges of both oxygen and hydrogen atoms within $(H_2O)_2$ shown in Figure 10. Similar results are obtained for the systems $(H_2O)_n$ with $n=3–6$, as can be observed throughout Tables S1–S4 in the Supporting Information.

Another interesting feature that emerges from the comparison of V_{cl} and V_X is that in general $|V_{cl}^{AB}| > |V_X^{AB}|$ for a given pair of atoms A and B. Nonetheless, $|V_X|$ is considerably larger than $|V_{cl}|$ for the interactions among water molecules, as can be seen in Figure 8. This means that there is a considerable cancellation of terms within the classical interaction energy in opposition to the exchange component in which all the atomic pairwise contributions are attractive.[91]

In contrast to the classical part of the interaction energy, the only relevant contributions to the exchange component come from the pairs formed among the atoms directly involved in the hydrogen bonding, that is, O−H···O. The magnitude of the exchange energy between contiguous oxygen atoms per water molecule, $V_X(O···O)$,[1] increases with the size of the system as shown in Figure 11. The same trend is observed for $V_X(O···H)_{bonding}$ that is, the exchange interaction between an accepting oxygen and the corresponding hydrogen-bonding atom. This observation is concordant with the description of bond paths as favored exchange channels between two atoms,[41] which implies that the electrostatic fields that control the redistribution of charge in the formation of a hydrogen bond modify the electronic structure in such a way that the electron delocalization between water molecules is enhanced. In this regard, Table 3 shows the delocalization indexes between neighboring O atoms,

Table 3. Localization and delocalization indexes involving the oxygen and hydrogen-bonding atoms in small $(H_2O)_n$ clusters with $n=2–6$. Intra- and intermolecular delocalization indexes between A and B are denoted by $\delta(A−B)$ and $\delta(A···B)$, respectively. The delocalization among water molecules is reported as well. Atomic units are used throughout.

n	$\lambda(O)$	$\lambda(H_{bonding})$	$\delta(O−H_{bonding})$	$\delta(O···H_{bonding})$	$\delta(O···O)$	$\delta(H_2O···H_2O)$
2	8.6799	0.0407	0.4823	0.0596	0.0669	0.1307
3	8.7034	0.0365	0.4549	0.0605	0.0756	0.1414
4	8.7173	0.0308	0.4028	0.0797	0.0977	0.1827
5	8.7211	0.0291	0.3884	0.0826	0.1030	0.1910
6	8.7257	0.0284	0.3828	0.0829	0.1048	0.1933

$\delta(O···O)$, an O and an H atom connected by a hydrogen bond, $\delta(O···H_{bonding})$, and adjacent water molecules, $\delta(H_2O···H_2O)$, for the water clusters considered in this work. The three delocalization indexes increase with the size of the cluster, which means that the cooperative effects of hydrogen bonding in small water clusters are accompanied by an increment in the number of delocalized electrons in these cyclic structures. This is to say that cooperativity of hydrogen bonding within $(H_2O)_n$ clusters emerges due to the opening of an exchange (i.e., delocalization) channel inside the cyclic structures of these systems. The reduction in the electron population of $H_{bonding}$ occurs with a decrease in the fraction of localized electrons of the bonding hydrogen atom ($\lambda(H_{bonding})/N(H_{bonding})$) and an accompanying rise in the number of available delocalized electrons. The corresponding quotient for the oxygen atoms, $\lambda(O)/N(O)$, remains nearly invariant as water molecules are added to the system. The augmentation of the delocalization indices in Table 3 is in accordance with the fact that the electron density at the bond critical point (bcp) associated with the hydrogen bonding increases with the number of water molecules in the cluster as shown in Table 1. The tendencies observed in $V_X(O···O)$, $V_X(O···H)$, and $\rho(O···H)$ indicate an enhancement of the covalent character of the interaction among the atoms that participate in the hydrogen bonds

---

[1] The notation $V_\sigma(A···B)$ ($V_\sigma(A−B)$), in which σ indicates either the correlation, exchange, exchange-correlation, or coulombic components of the electron–electron interaction, denote V_σ^{AB} in the intermolecular (intramolecular) interaction of the pair of atoms A and B; the same notation is used to indicate the delocalization index $\delta(A,B)$.

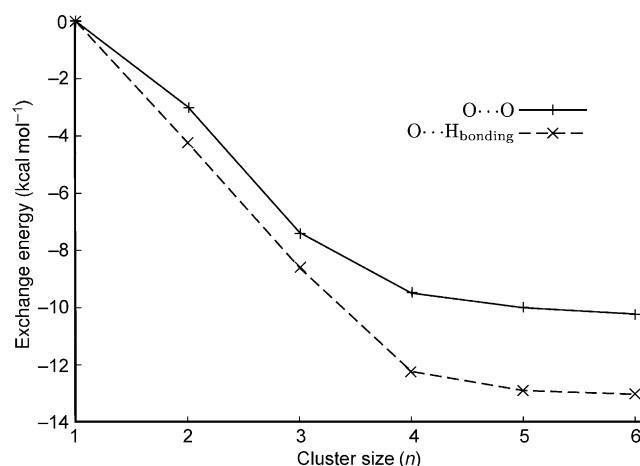under consideration as water molecules are added to the system. This rise in covalency in addition to the aforementioned behavior of electrostatic, polarization, and charge-transfer effects determine the cooperative effects in the network of hydrogen bonds of $(H_2O)_2$ and cyclic $(H_2O)_n$ with $n = 3–6$.

Relative importance of first and second neighbors and intramolecular interactions: To study the relative significance of the interactions between first and second neighbors, the total exchange and classic contributions to the interaction energy per water molecule were compared with the corresponding values obtained by taking into account only contiguous molecules. The results are shown in Figure 12, and they indicate that the exchange component depends almost com-
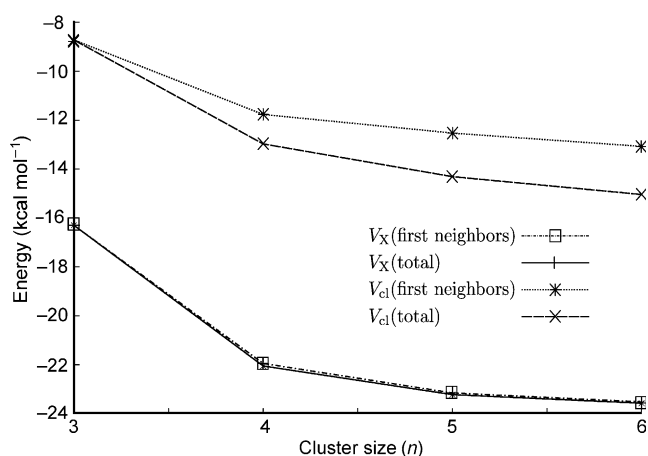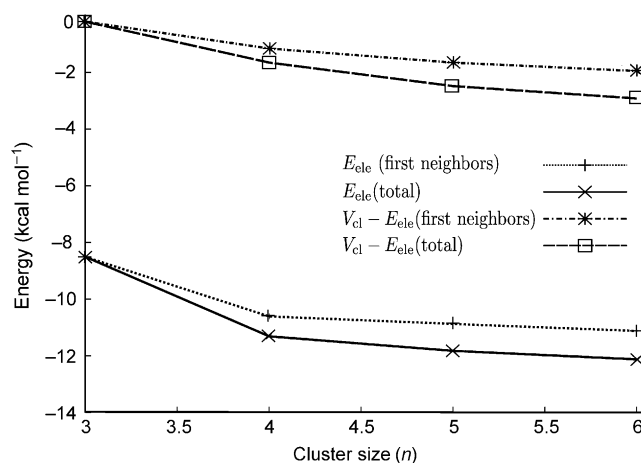

Figure 13. Electrostatic and the difference between the classical and the electrostatic contributions per water molecule in clusters $(H_2O)_n$ in which $n = 2–6$. The plots were obtained by considering the interactions among all the monomers in the clusters and only between first neighbors.
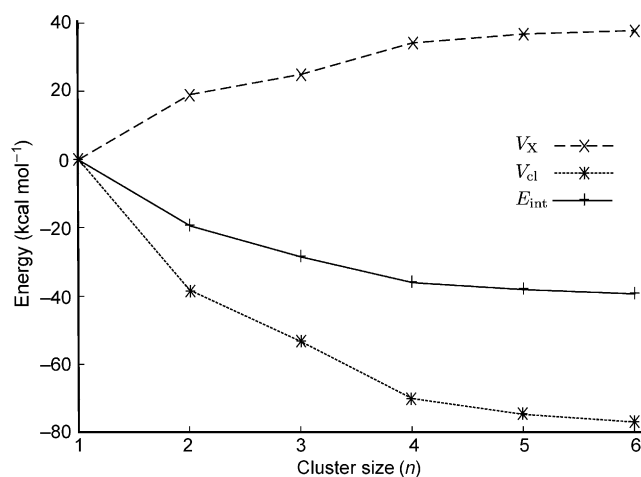

Figure 12. Classical and exchange energies per water molecule within small water clusters $(H_2O)_n$ with $n = 2–6$ considering the interactions within all the monomers and only between first neighbors.

Figure 14. Average classical and exchange intramolecular interaction energies associated with the covalent bond O−H$_{bonding}$ as a function of the system size for small water clusters $(H_2O)_n$ in which $n = 2–6$. The corresponding values for an isolated water molecule are used as reference.

pletely upon the interactions among first neighbors in contrast with the classical component in which the effects of second and further neighbors become more important as the size of the cluster is increased. The classical interactions among third neighbors in the ring water hexamer are also important, as can be seen in Table S4 of the Supporting Information. The electrostatic components as well as the polarization and charge-transfer effects are also affected by second and more distant neighbors as shown in Figure 13. These parts of the interaction energy also have an important contribution from second neighbors in a similar fashion to V_{cl}. The behavior observed in Figures 12 and 13 is consistent with the description of exchange as a short-range energy, whereas electrostatics and polarization are considered long-range interactions.[91]

The most relevant intramolecular interaction within the water dimer and cyclic $(H_2O)_n$ clusters with $n = 3–6$ is the covalent bond O−H$_{bonding}$. Figure 14 shows the interaction energy associated with this pair of atoms as well as its classical and exchange parts. Since the H$_{bonding}$ (O) atoms acquire a more positive (negative) charge as the size of the water

cluster is increased (see Table 1), it is expected that V_{cl}(O−H$_{bonding}$) is more stabilizing as water molecules are added to the system. On the other hand, the magnitude of the exchange component of the interaction between O and H$_{bonding}$, $|V_X$(O−H$_{bonding}$)$|$ decreases as water molecules are incorporated into the molecular cluster. This is consistent with the fact that both the delocalization index between the oxygen atom and H$_{bonding}$, δ(O−H)$_{bonding}$, as well as the electron density at the bcp associated with the bond path that links this pair of atoms ρ_{bcp}(O−H$_{bonding}$) decrease monotonically from a water molecule to $(H_2O)_6$ as indicated in Tables 1 and 3. Despite the increase in the interaction energy for the pair O and H$_{bonding}$ as the size of the system is increased, the reduction of $|V_X$(O−H)$_{bonding}|$, δ(O−H)$_{bonding}$, and ρ_{bcp}(O−H$_{bonding}$) point to a diminished covalent character of the O−H$_{bonding}$ with the addition of water molecules. Thus,

the cooperative effects of the hydrogen bonding within small water clusters are in agreement with the notion that the hydrogen bond X−H···Y entails a proton donation to Y in which the average of the electron pairs associated with the bonding X−H, and therefore the covalent character of the interaction is reduced.

Now that we have considered both intra- and intermolecular interactions that involve $H_{bonding}$ atoms, it is instructive to examine the splitting of the electron population of atoms in localized and delocalized electrons [Eq. (6)]:

$$N(\Omega) = \lambda(\Omega) + \frac{1}{2}\sum_{\Omega' \neq \Omega} \delta(\Omega, \Omega') \tag{6}$$

By taking account of the most important interactions of the O and $H_{bonding}$, one gets [Eq. (7) and Eq. (8)]:

$$N(H_{bonding}) \approx \lambda(H_{bonding}) + \frac{1}{2}(\delta(O - H_{bonding})$$
$$+\delta(O \cdots H_{bonding})) \tag{7}$$

$$N(O) \approx \lambda(O) + \frac{1}{2}(\delta(O - H_{free}) + \delta(O - H_{bonding})$$
$$+\delta(O \cdots H_{bonding}) + \delta(O \cdots O') + \delta(O \cdots O'')) \tag{8}$$

in which O′ and O″ are oxygen atoms that interact with O through a hydrogen bond. The term in the RHS of Equation (7) that decreases the most as water molecules are added to the system is $\delta(O-H)_{bonding})$, whereas the terms with increase preponderantly in the RHS of Equation (8) are $\lambda(O)$, $\delta(O\cdots O'')$, and $\delta(O\cdots H)_{bonding})$. This means that electron density is removed from the covalent bond O−$H_{bonding}$ to increase the number of electrons involved in the hydrogen bond and those localized on the oxygen, thereby enhancing the basicity of this atom. In other words, the polarization of O and $H_{bonding}$ is accompanied by a rise in the number of delocalized electrons throughout the cyclic structure of small water clusters, that is, there is a polarization-assisted delocalization process associated with the cooperative effects of hydrogen bonding within these systems. This view is supported by the analysis of the local charge concentrations around the oxygen atom given by the local minima of $\nabla^2\rho(\mathbf{r})$ presented in Table 4. As water molecules are added to the system, the magnitude of $\nabla^2\rho(\mathbf{r})$ becomes smaller at the local charge concentrations that correspond to the hydrogen bonds, which suggests a reduction in the domain associated with these lone pairs, that is, a closer similarity to bonded pairs and a consequent strengthening of the

$O\cdots H_{bonding}$ interactions. On the contrary, the magnitude of the local charge concentrations associated with the covalent bond O−$H_{bonding}$ increases when the size of the system is enlarged, thereby indicating that the domains of such electron pairs are more extensive, and thus, they more closely resemble those of lone pairs. This reflects the decrease in the covalent character of the O−$H_{bonding}$ interaction with a more pronounced difference in the electronegativity of the O and $H_{bonding}$ atoms as more water molecules are contained within the system.

Conclusion

The IQA approach and the QTAIM topological analysis of the electron density have been used to study the cooperative effects of hydrogen bonding in small cyclic water clusters $(H_2O)_n$ with $n=2$–6. In addition, the electrostatic component of the interaction energy was calculated using one and two-electron integrals, thereby evading convergence issues related with multipolar expansions. The IQA partition energy shows that the cooperative effects of hydrogen bonding in small water clusters result from a compromise between the deformation energy of the constituting water molecules and the interaction energy among these monomers, in which both increase in magnitude with the size of the system, but the interaction energy becomes more dominant as the molecular cluster is enlarged. Furthermore, the electrostatic, polarization, charge transfer, and exchange become more attractive with the inclusion of water molecules in the studied clusters, and the most important contribution to E_{int} is V_X, which is in opposition to the traditional viewpoint that hydrogen bonding in water is an electrostatically driven intermolecular interaction. The IQA exchange energies together with selected QTAIM charges and $\delta(A,B)$ indices, as well as the study of the electron density at relevant bond critical points indicate the important role of polarization and electron delocalization in the cooperative effects of hydrogen bonding in water clusters. The analysis of these quantities bespeaks the augmentation of the covalent character of hydrogen bonds as more water molecules are included in the system and the opposite behavior of the covalent bond O−$H_{bonding}$. Overall, different insights are offered about the cooperative effects of hydrogen bonding in small cyclic water clusters, which could be useful in future studies about this important interaction.

Appendix: Evaluation of the electrostatic energy E_{ele}

We describe in this appendix the evaluation of the electrostatic energy, E_{ele}, in Equation (4). In this work, all the fragment electron densities $\rho^{\mathscr{I}}(\mathbf{r})$ are expressed in terms of a common one-particle basis set of real functions [Eq. (9)]:

$$\rho^{\mathscr{I}}(\mathbf{r}) = \sum_{\mu\nu} D^{\mathscr{I}}_{\mu\nu}\chi_\nu(\mathbf{r})\chi_\mu(\mathbf{r}) \tag{9}$$

Table 4. Minima of $\nabla^2\rho(\mathbf{r})$ associated with 1) the covalent bonds O−$H_{bonding}$ and 2) the hydrogen bonds within small water clusters $(H_2O)_n$, with $n=2$–6.

n	O−$H_{bonding}$	O···$H_{bonding}$
2	−3.1589	−4.7801
3	−3.1864	−4.5402
4	−3.2896	−4.4634
5	−3.3324	−4.4515
6	−3.3515	−4.4506

When substituting Equation (9) in the expression of the total electron density [Eq. (10)]:

$$\rho_T^{\mathscr{I}}(\mathbf{r}) = \sum_{A \in \mathscr{I}} Z_A \partial(\mathbf{r} - \mathbf{r}_A) - \rho^{\mathscr{I}}(\mathbf{r}) \tag{10}$$

and $\rho_T^{\mathscr{G}}(\mathbf{r})$ and $\rho_T^{\mathscr{H}}(\mathbf{r})$ in Equation (4), we have [Eq. (11)]:

$$E_{\text{ele}} = V_{\text{nn}}^{\mathscr{G}\mathscr{H}} + \text{tr}\mathbf{D}^{\mathscr{G}}\mathbf{h}^{\mathscr{H}} + \text{tr}\mathbf{D}^{\mathscr{H}}(\mathbf{h}^{\mathscr{G}} + \mathbf{J}^{\mathscr{G}}) \tag{11}$$

in which $(\mathbf{D}^{\mathscr{I}})_{\mu\nu}$, $(D_{\mu\nu}^{\mathscr{I}})$, $V_{\text{nn}}^{\mathscr{G}\mathscr{H}} = \Sigma_{A \in \mathscr{G}, B \in \mathscr{H}} Z_A Z_B r_{AB}^{-1}$, $(\mathbf{h}^{\mathscr{I}})_{\mu\nu} = -\Sigma_{A \in \mathscr{I}} Z_A h_{\mu\nu}^A$, $(\mathbf{J}^{\mathscr{I}})_{\mu\nu} = \Sigma_{\sigma\tau} D_{\sigma\tau}^{\mathscr{I}} O_{\tau\sigma\mu\nu}$, and $h_{\mu\nu}^X$ and $O_{\mu\nu\sigma\tau}$ are the basic one- and two-electron integrals, respectively, defined as [Eq. (12) and (13)]:

$$h_{\mu\nu}^X = \int \chi_\mu(\mathbf{r}_1)\chi_\nu(\mathbf{r}_1)|\mathbf{r}_1 - \mathbf{r}_X|^{-1}\mathrm{d}\mathbf{r}_1 \tag{12}$$

$$O_{\mu\nu\sigma\tau} = \int\int \chi_\mu(\mathbf{r}_1)\chi_\nu(\mathbf{r}_1)\mathbf{r}_{12}^{-1}\chi_\sigma(\mathbf{r}_2)\chi_\tau(\mathbf{r}_2)\mathrm{d}\mathbf{r}_1\mathrm{d}\mathbf{r}_2 \tag{13}$$

Therefore, the electrostatic energy between two molecules $\mathscr{G}$ and $\mathscr{H}$ is calculated as the sum of the repulsion between the nuclei, ($V_{\text{nn}}^{\mathscr{G}\mathscr{H}}$), the attraction between the electrons of $\mathscr{G}$ and the nuclei of $\mathscr{H}$ (tr $\mathbf{D}^{\mathscr{G}}\mathbf{h}^{\mathscr{H}}$), the attraction between the electrons of $\mathscr{H}$ and the nuclei of $\mathscr{G}$ (tr $\mathbf{D}^{\mathscr{H}}\mathbf{h}^{\mathscr{G}}$), and the interaction between the electrons of $\mathscr{G}$ and $\mathscr{H}$ (tr $\mathbf{D}^{\mathscr{H}}\mathbf{J}^{\mathscr{G}}$).

Acknowledgements

[1] J. D. Watson, F. H. Crick, *Nature* **1953**, *171*, 737.
[2] L. Pauling, R. B. Corey, *Proc. Natl. Acad. Sci. USA* **1951**, *37*, 251.
[3] L. Pauling, R. B. Corey, *Proc. Natl. Acad. Sci. USA* **1951**, *37*, 261.
[4] J.-M. Lehn, *Angew. Chem.* **1988**, *100*, 91; *Angew. Chem. Int. Ed. Engl.* **1988**, *27*, 89.
[5] G. R. Desiraju, *Acc. Chem. Res.* **2002**, *35*, 565.
[6] E. Arunan, G. R. Desiraju, R. a. Klein, J. Sadlej, S. Scheiner, I. Alkorta, D. C. Clary, R. H. Crabtree, J. J. Dannenberg, P. Hobza, H. G. Kjaergaard, A. C. Legon, B. Mennucci, D. J. Nesbitt, *Pure Appl. Chem.* **2011**, *83*, 1637.
[7] T. Steiner, *Angew. Chem.* **2002**, *114*, 50; *Angew. Chem. Int. Ed.* **2002**, *41*, 48.
[8] R. Ludwig, *Angew. Chem.* **2001**, *113*, 1856; *Angew. Chem. Int. Ed.* **2001**, *40*, 1808.
[9] S. Scheiner, *Hydrogen Bonding: A Theoretical Perspective*, Oxford University Press, New York, **1997**.
[10] K. Hermansson, M. Alfredsson, *J. Chem. Phys.* **1999**, *111*, 1993.
[11] L. Albrecht, R. J. Boyd, *J. Phys. Chem. A* **2012**, *116*, 3946.
[12] M. Devereux, P. L. A. Popelier, *J. Phys. Chem. A* **2007**, *111*, 1536.
[13] M. C. Das, S. B. Maity, P. K. Bharadwaj, *Curr. Opin. Solid State Mater. Sci.* **2009**, *13*, 76.
[14] C. Pérez, M. T. Muckle, D. P. Zaleski, N. A. Seifert, B. Temelso, G. C. Shields, Z. Kisiel, B. H. Pate, *Science* **2012**, *336*, 897.
[15] Y. Wang, V. Babin, J. M. Bowman, F. Paesani, *J. Am. Chem. Soc.* **2012**, *134*, 11116.
[16] K. Liu, J. D. Cruzan, R. J. Saykally, *Science* **1996**, *271*, 929.
[17] N. Pugliano, R. Saykally, *J. Chem. Phys.* **1992**, *96*, 1832.
[18] N. Pugliano, R. Saykally, *Science* **1992**, *257*, 1937.
[19] J. D. Cruzan, L. B. Braly, K. Liu, M. G. Brown, J. G. Loeser, R. J. Saykally, *Science* **1996**, *271*, 59.
[20] K. Liu, M. G. Brow, J. D. Cruzan, R. J. Saykally, *Science* **1996**, *271*, 62.
[21] J. K. Gregory, D. C. Clary, K. Liu, M. G. Brown, R. J. Saykally, *Science* **1997**, *275*, 814.
[22] S. S. Xantheas, T. H. Dunning, *J. Chem. Phys.* **1993**, *99*, 8774.
[23] C. E. Kolb, J. T. Dayne, D. R. Wornsnop, M. J. Molina, R. T. Meads, A. A. Viggiano, *J. Am. Chem. Soc.* **1994**, *116*, 10314.
[24] K. Morokuma, C. Muguruma, *J. Am. Chem. Soc.* **1994**, *116*, 10316.
[25] H. R. Carlon, *J. Phys. D* **1984**, *17*, 1221.
[26] H. R. Carlon, *J. Appl. Phys.* **1981**, *52*, 2638.
[27] H. R. Carlon, *Infrared Phys.* **1979**, *19*, 549.
[28] H. R. Carlon, *J. Appl. Phys.* **1981**, *52*, 3111.
[29] Y. Ma, P. Politzer, *Int. J. Mol. Sci.* **2004**, *5*, 130.
[30] E. D. Glendening, *J. Phys. Chem. A* **2005**, *109*, 11936.
[31] M. P. Mitoraj, A. Michalak, T. Ziegler, *J. Chem. Theory Comput.* **2009**, *5*, 962.
[32] R. Z. Khaliullin, A. T. Bell, M. Head-Gordon, *Chem. Eur. J.* **2009**, *15*, 851.
[33] V. A. Mora-Gómez, Bachelor Thesis, National Autonomous University of Mexico (Mexico), **2013**.
[34] M. Swart, M. Sola, F. M. Bickelhaupt, *J. Comput. Chem.* **2011**, *32*, 1117.
[35] G. Hincapié, N. Acelas, M. Castaño, J. David, A. Restrepo, *J. Phys. Chem. A* **2010**, *114*, 7809.
[36] C. J. Tainter, J. L. Skinner, *J. Chem. Phys.* **2012**, *137*, 104304.
[37] K. Szalewicz, C. Leforestier, A. van der Avoird, *Chem. Phys. Lett.* **2009**, *482*, 1.
[38] Y. Wang, X. Huang, B. C. Shepler, B. J. Braams, J. M. Bowman, *J. Chem. Phys.* **2011**, *134*, 094509.
[39] M. A. Blanco, Á. Martín Pendás, E. Francisco, *J. Chem. Theory Comput.* **2005**, *1*, 1096.
[40] E. Francisco, Á. Martín Pendás, M. Blanco, *J. Chem. Theory Comput.* **2006**, *2*, 90.
[41] Á. Martín Pendás, E. Francisco, M. A. Blanco, C. Gatti, *Chem. Eur. J.* **2007**, *13*, 9362.
[42] Á. Martín Pendás, E. Francisco, M. Blanco, *Chem. Phys. Lett.* **2007**, *437*, 287.
[43] Á. Martín Pendás, E. Francisco, M. Blanco, *J. Phys. Chem. A* **2006**, *110*, 12864.
[44] A. Martín Pendás, M. A. Blanco, E. Francisco, *J. Comput. Chem.* **2009**, *30*, 98.
[45] V. Tognetti, L. Joubert, *J. Chem. Phys.* **2013**, *138*, 024102.
[46] A. Martín Pendás, M. A. Blanco, E. Francisco, *J. Chem. Phys.* **2006**, *125*, 184112.
[47] J. Passmore, J. M. Rautiainen, *Eur. J. Inorg. Chem.* **2012**, 6002.
[48] T. I. Madzhidov, G. A. Chmutova, A. Martín Pendás, *J. Phys. Chem. A* **2011**, *115*, 10069.
[49] P. Dem'yanov, P. Polestshuk, *Chem. Eur. J.* **2012**, *18*, 4982.
[50] D. Tiana, E. Francisco, M. A. Blanco, P. Macchi, A. Sironi, A. Martín Pendás, *J. Chem. Theory Comput.* **2010**, *6*, 1064.
[51] D. Tiana, E. Francisco, M. A. Blanco, P. Macchi, A. Sironi, A. Martín Pendás, *Phys. Chem. Chem. Phys.* **2011**, *13*, 5068.
[52] F. Cortés-Guzmán, R. F. W. Bader, *Coord. Chem. Rev.* **2005**, *249*, 633.
[53] S. M. Lapointe, S. Farrag, H. J. Bohórquez, R. J. Boyd, *J. Phys. Chem. B* **2009**, *113*, 10957.
[54] L. J. Farrugia, C. Evans, M. Tegel, *J. Phys. Chem. A* **2006**, *110*, 7952.
[55] P. B. Coto, D. Roca-Sanjuán, L. Serrano-Andrés, A. Martín Pendás, S. Martí, J. Andrés, *J. Chem. Theory Comput.* **2009**, *5*, 3032.
[56] *The Quantum Theory of Atoms in Molecules: From Solid State to DNA and Drug Design* (Eds.: C. F. Matta, R. J. Boyd), Wiley-VCH, Weinheim, **2007**.
[57] R. F. W. Bader, *J. Phys. Chem. A* **1998**, *102*, 7314.
[58] C. F. Matta, J. Hernández-Trujillo, T.-H. Tang, R. F. W. Bader, *Chem. Eur. J.* **2003**, *9*, 1940.
[59] J. Hernández-Trujillo, C. F. Matta, *Struct. Chem.* **2007**, *18*, 849.
[60] J. Poater, M. Solà, F. M. Bickelhaupt, *Chem. Eur. J.* **2006**, *12*, 2889.

[61] R. F. W. Bader, *Atoms in Molecules: A Quantum Theory*, Oxford University Press, Oxford, **1995**.

[62] T. A. Keith, *AIMAll, Version 12.06.03*, TK Gristmill Software, Overland Park KS, USA, **2012**, aim.tkgristmill.com.

[63] R. F. W. Bader, M. E. Stephens, *J. Am. Chem. Soc.* **1975**, *97*, 7391.

[64] R. F. W. Bader, A. Streitwieser, A. Neuhaus, K. E. Laidig, P. Speers, *J. Am. Chem. Soc.* **1996**, *118*, 4959.

[65] X. Fradera, M. A. Austen, R. F. W. Bader, *J. Phys. Chem. A* **1999**, *103*, 304.

[66] F. L. Hirshfeld, *Theor. Chim. Acta* **1977**, *44*, 129.

[67] A. D. Becke, *J. Chem. Phys.* **1988**, *88*, 2547.

[68] A. Martín Pendás, E. Francisco, M. A. Blanco, *J. Comput. Chem.* **2005**, *26*, 344.

[69] T. Rocha-Rinza, J. Hernández-Trujillo, *Chem. Phys. Lett.* **2006**, *422*, 36.

[70] C. Esterhuysen, G. Frenking, *Theor. Chem. Acc.* **2004**, *111*, 381.

[71] G. Frenking, *Coord. Chem. Rev.* **2003**, *238–239*, 55.

[72] F. M. Bickelhaupt, J. E. Baerends, *Rev. Comput. Chem.* **2000**, *15*, 1.

[73] T. Ziegler, A. Rauk, *Inorg. Chem.* **1979**, *18*, 1755.

[74] T. Ziegler, A. Rauk, *Inorg. Chem.* **1979**, *18*, 1558.

[75] C. Møller, M. S. Plesset, *Phys. Rev.* **1934**, *46*, 618.

[76] T. H. Dunning, *J. Chem. Phys.* **1989**, *90*, 1007.

[77] M. W. Schmidt, K. K. Baldridge, J. A. Boatz, S. T. Elbert, M. S. Gordon, J. H. Jensen, S. Koseki, N. Matsunaga, K. A. Nguyen, S. Su, T. L. Windus, M. Dupuis, J. A. Montgomery, *J. Comput. Chem.* **1993**, *14*, 1347.

[78] A. D. Boese, G. Jansen, M. Torheyden, S. Höfener, W. Klopper, *Phys. Chem. Chem. Phys.* **2011**, *13*, 1230.

[79] J. Segarra-Martí, M. Merchán, D. Roca-Sanjuán, *J. Chem. Phys.* **2012**, *136*, 244306.

[80] A. Martín Pendás, E. Francisco, *Promolden, A QTAIM/IQA code*, unpublished.

[81] M. García-Revilla, E. Francisco, A. Costales, A. Martín Pendás, *J. Phys. Chem. A* **2012**, *116*, 1237.

[82] H.-J. Werner, P. J. Knowles, G. Knizia, F. R. Manby, M. Schütz, P. Celani, T. Korona, R. Lindh, A. Mitrushenkov, G. Rauhut, K. R. Shamasundar, T. B. Adler, R. D. Amos, A. Bernhardsson, A. Berning, D. L. Cooper, M. J. O. Deegan, A. J. Dobbyn, F. Eckert, E. Goll, C. Hampel, A. Hesselmann, G. Hetzer, T. Hrenar, G. Jansen, C. Köppl, Y. Liu, A. W. Lloyd, R. A. Mata, A. J. May, S. J. McNicholas, W. Meyer, M. E. Mura, A. Nicklaß, D. P. O'Neill, P. Palmieri, D. Peng, K. Pflüger, R. Pitzer, M. Reiher, T. Shiozaki, H. Stoll, A. J. Stone, R. Tarroni, T. Thorsteinsson, M. Wang, *MOLPRO, Version 2012.1, a Package of ab initio Programs*, **2012**, http://www.molpro.net.

[83] T. Williams, C. Kelley, *Gnuplot 4.2: An Interactive Plotting Program*, **2010**, http://gnuplot.sourceforge.net/.

[84] M. D. Hanwell, D. E. Curtis, D. C. Lonie, T. Vandermeersch, E. Zurek, G. R. Hutchison, *J. Cheminform.* **2012**, *4*, 17.

[85] T. Helgaker, P. Jørgensen, J. Olsen, *Molecular Electronic Structure Theory*, Wiley, Chichester, **2004**.

[86] S. A. Clough, Y. Beers, G. Klein, L. Rothman, *J. Chem. Phys.* **1973**, *59*, 2254.

[87] Y. S. Badyal, M.-L. Saboungi, D. L. Price, S. D. Shastri, D. R. Haeffner, a. K. Soper, *J. Chem. Phys.* **2000**, *112*, 9206.

[88] P. Silvestrelli, M. Parrinello, *Phys. Rev. Lett.* **1999**, *82*, 3308.

[89] G. Chałasiński, M. M. Szczśniak, P. Cieplak, S. Scheiner, *J. Chem. Phys.* **1991**, *94*, 2873.

[90] A. Milet, R. Moszynski, U. M. R. C. Ulp, I. L. Bel, P. E. S. Wormer, A. V. D. Avoird, *J. Phys. Chem. A* **1999**, *103*, 6811.

[91] A. J. Stone, *The Theory of Intermolecular Forces*, Oxford University Press, Oxford, **1997**.